Thermally driven Marangoni surfers

Alois Würger

HAL Id: hal-01021962
https://hal.science/hal-01021962

Thermally driven Marangoni surfers

Alois Würger[1] †

[1]Laboratoire Ondes et Matière d'Aquitaine, Université de Bordeaux–CNRS, 33405 Talence, France

We study auto-propulsion of a interface particle, which is driven by the Marangoni stress arising from a self-generated asymmetric temperature or concentration field. We calculate separately the long-range Marangoni flow $\boldsymbol{v}^I$ due to the stress discontinuity at the interface and the short-range velocity field $\boldsymbol{v}^P$ imposed by the no-slip condition on the particle surface; both contributions are evaluated for a spherical floater with temperature monopole and dipole moments. We find that the self-propulsion velocity is given by the amplitude of the "source doublet" which belongs to short-range contribution $\boldsymbol{v}^P$. Hydrodynamic interactions, on the other hand, are determined by the long-range Marangoni flow $\boldsymbol{v}^I$; its dipolar part results in an asymmetric advection pattern of neighbor particles, which in turn may perturb the known hexatic lattice or even favor disordered states.

1. Introduction

Autonomous motion is an important issue in active soft matter, with possible applications ranging from energy harvesting (Okawa et al. 2009) to microfluidic transport (Robert de Saint Vincent & Delville 2012) and mixing (Venancio-Marques et al. 2013). Recently realized microswimmers carry, as active element, heat-absorbing or catalytic parts which generate temperature or concentration gradients in the surrounding liquid. For particles dispersed in bulk phases, these thermodynamic forces give rise to an effective slip velocity, which in turn implies self-propulsion at a speed of the order of ten microns per second (Paxton et al. 2005; Qian et al. 2013).

Much higher velocities can be achieved for active particles trapped at a liquid interface, where the self-generated temperature or concentration gradient induces a non-uniform interface tension and a Marangoni flow. Upon laser-heating one side of a centimeter-size object floating on water, Okawa et al. (2009) observed self-propulsion at several cm/s. The mutual Marangoni advection of camphor releasing gel particles results in dynamical self assembly (Soh et al. 2008)

Recent theoretical studies dealt with Marangoni propulsion due to a non-uniform surfactant concentration. The resulting Marangoni stress comprises a dipolar term that is proportional to the inverse distance from its source. Thus Lauga & Davis (2012) calculated the Marangoni flow for an asymmetric active disk, whereas Masoud & Stone (2014) considered the motion of ellipsoidal particles in terms of a reciprocal theorem. Accounting for advective non-linearities in the surfactant concentration, Nagai et al. (2013) found spontaneous rotation of particles floating on a liquid droplet.

In the present paper we consider Marangoni propulsion driven by a non-uniform temperature or bulk concentration field, the dipolar term of which decays with the square of inverse distance. Assuming small Reynolds, Marangoni, Péclet, and capillary numbers, we rely on Stokes' equation, linearize the field dependent tension, and neglect the interface deformation. For a spherical particle with an off-center heat source, we calculate

† Email address for correspondence: a.wuerger@loma.u-bordeaux1.fr

A. Würger
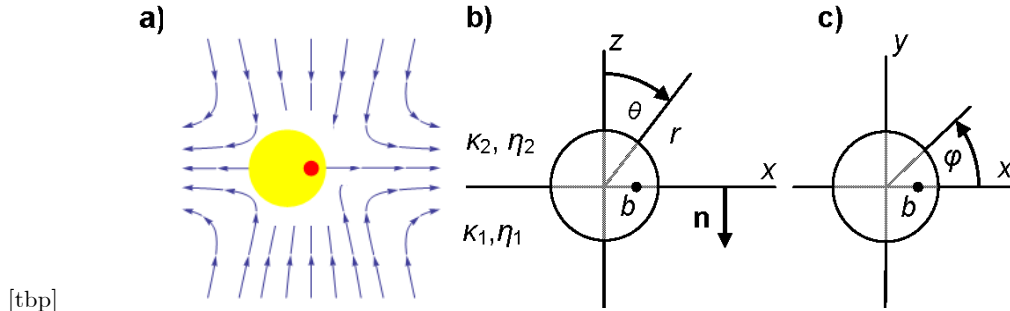
FIGURE 1. Schematic view of a trapped particle with an off-center active spot. a) The Marangoni flow is symmetric with respect to the hot spot, yet not with respect to the particle center. b) Side view of a particle at a fluid interface separating phases 1 and 2 with thermal conductivity κ_i and viscosity η_i. The polar angle θ is defined with respect to the z-axis. c) Top view with the azimuthal angle φ. The idealized heat source is indicated by the black point at a distance b from the particle center.

both the long-range Marangoni flow $\boldsymbol{v}^I$ driven by the non-uniform interface tension and the short-range velocity $\boldsymbol{v}^P$ imposed by no-slip condition on the particle surface.

2. Marangoni effect and boundary conditions

Consider a colloidal particle trapped at a liquid interface. For the sake of simplicity we discuss a sphere that is trapped at midplane, as shown in Fig. 1. Retaining the first two terms of the multipole expansion of the temperature profile we find

$$T(r) = T_0 + \frac{Q}{2\pi\bar{\kappa}}\left(\frac{1}{r} + \frac{\boldsymbol{b}\cdot\boldsymbol{r}}{r^3} + ...\right) \tag{2.1}$$

where Q is the total power absorbed by the particle and $\bar{\kappa} = \kappa_1 + \kappa_2$ the sum of the thermal conductivities of the lower and upper fluid phases. The strength and orientation of the dipole term are given by the position of the absorption area with respect to the particle center, $\boldsymbol{b} = b\boldsymbol{e}_x$, as shown in Fig. 1 for a point-like heat source. Moreover, b depends on the conductivity contrast of the particle and fluid phases. In the case of a chemical Marangoni effect, T and κ are the solute concentration and diffusivity in the fluid phases and Q is the chemical activity at the particle surface.

The thermal gradient induces a Marangoni flow along the liquid interface. The temperature dependence of the interface tension, $\gamma_T = d\gamma/dT$, results in the hydrodynamic boundary condition

$$(1 - \boldsymbol{nn})\cdot\left(\boldsymbol{\sigma}^M\cdot\boldsymbol{n} + \gamma_T\boldsymbol{\nabla}T\right) = 0, \tag{2.2}$$

where $\boldsymbol{\sigma}^M = \boldsymbol{\sigma}^{(1)} - \boldsymbol{\sigma}^{(2)}$ is the stress discontinuity across the interface, $\boldsymbol{n}$ the (downward oriented) normal vector, and $\boldsymbol{\nabla}\gamma = \gamma_T\boldsymbol{\nabla}T$ the tension gradient. The stress tensor $\boldsymbol{\sigma}$ comprises viscous and pressure terms, $\sigma_{ij} = \eta(\partial_i v_j + \partial_j v_i) - P\delta_{ij}$, with the velocity components v_i and where the viscosity η takes values η_1 and η_2 in the two phases. The fluid velocity is continuous at the interface, and its normal component must vanish,

$$\boldsymbol{v}\cdot\boldsymbol{n}|_I = 0. \tag{2.3}$$

One more boundary condition is provided by the no-slip condition at the particle surface,

$$\boldsymbol{v}|_P = \boldsymbol{u}, \tag{2.4}$$

where $\boldsymbol{v}(\boldsymbol{r})$ is the velocity field of the fluid and $\boldsymbol{u}$ the particle velocity, which is necessarily parallel to the interface.

Since there are no external body forces acting on the particle we have

$$\oint \mathrm{d}\boldsymbol{s}\gamma + \oint \mathrm{d}\boldsymbol{S} \cdot \boldsymbol{\sigma} = 0, \qquad (2.5)$$

where the first term gives the net force exerted by the surface tension along the contact line with element $\mathrm{d}\boldsymbol{s}$, and the second one, the surface integral of the stress tensor with the oriented surface element $\mathrm{d}\boldsymbol{S}$.

For later convenience we rewrite the above conditions for the velocity and stress components in spherical coordinates. With the axes defined in Fig. 1 we have $\boldsymbol{n} = \boldsymbol{e}_\theta$ and

$$(1 - \boldsymbol{nn}) \cdot \boldsymbol{\sigma}^M \cdot \boldsymbol{n} = \boldsymbol{e}_r\sigma_{r\theta}^M + \boldsymbol{e}_\varphi\sigma_{\varphi\theta}^M. \qquad (2.6a)$$

Inserting the temperature gradient in (2.2), we find

$$\sigma_{r\theta}^M = \frac{\gamma_T Q}{2\pi\bar{\kappa}}\left(\frac{1}{r^2} + 2b\frac{\cos\varphi}{r^3}\right), \qquad \sigma_{\varphi\theta}^M = \frac{\gamma_T Q}{2\pi\bar{\kappa}}\frac{b\sin\varphi}{r^3}. \qquad (2.6b)$$

The zero normal velocity at the interface involves the polar component only,

$$v_\theta|_I = 0. \qquad (2.7)$$

Finally, imposing no-slip at the surface of the particle moving at velocity u along the x-axis, we have

$$v_r|_P = u\sin\theta\cos\varphi, \quad v_\theta|_P = u\cos\theta\cos\varphi, \quad v_\varphi|_P = -u\sin\varphi. \qquad (2.8)$$

The cosine $\cos\theta$ turns out to be a more convenient coordinate than the polar angle θ. Thus we use the shorthand notation

$$c = \cos\theta, \quad s = \sqrt{1 - c^2}.$$

Note that s is positive everywhere, whereas $c > 0$ and $c < 0$ on the upper and lower halfspaces, respectively.

Finally we note that the particle is not allowed to rotate about the horizontal axis. In other words, the point b in Fig. 1 is confined to the interface plane. This condition could be imposed through appropriate surface functionalization; it is satisfied, for example, if heating occurs through a small metal patch which itself is trapped at the fluid phase boundary.

3. Velocity field and stress tensor

The velocity field is solution of Stokes' equation $\eta\boldsymbol{\nabla}^2\boldsymbol{v} = \boldsymbol{\nabla}P$, which results in a set of coupled differential equations for the three velocity components $\boldsymbol{v} = v_r\boldsymbol{e}_r + v_\theta\boldsymbol{e}_\theta + v_\varphi\boldsymbol{e}_\varphi$ and the pressure P. With the vector Laplace operator one has

$$\Delta v_r - \frac{2v_r}{r^2} + \frac{2\partial_c(sv_\theta)}{r^2} - \frac{2\partial_\varphi v_\varphi}{sr^2} = \frac{\partial_r P}{\eta}, \qquad (3.1a)$$

$$\Delta v_\theta - \frac{v_\theta}{s^2r^2} - \frac{2s\partial_c v_r}{r^2} - \frac{2c\partial_\varphi v_\varphi}{s^2r^2} = -s\frac{\partial_c P}{\eta r}, \qquad (3.1b)$$

$$\Delta v_\varphi - \frac{v_\varphi}{s^2r^2} + \frac{2\partial_\varphi v_r}{sr^2} + \frac{2c\partial_\varphi v_\theta}{s^2r^2} = \frac{\partial_\varphi P}{\eta sr}, \qquad (3.1c)$$

where the derivative with respect to the polar angle is replaced according to $\partial_\theta = -s\partial_c$. The first term of each equation is given by the scalar Laplace operator

$$\Delta v_i = r^{-2}\partial_r(r^2\partial_r v_i) + r^{-2}\partial_c(s^2\partial_c v_i) + (sr)^{-2}\partial_\varphi^2 v_i. \qquad (3.1d)$$

Similarly, we have for the incompressibility condition

$$\boldsymbol{\nabla}\cdot\boldsymbol{v} = r^{-2}\partial_r(r^2 v_r) - r^{-1}\partial_c(sv_\theta) + (sr)^{-1}\partial_\varphi v_\varphi = 0. \qquad (3.1e)$$

For later use we give the components of the symmetrized stress in spherical coordinates,

$$\begin{aligned}
\sigma_{rr} &= 2\eta\partial_r v_r - P, \quad \sigma_{\theta\theta} = (2\eta/r)\left(-\partial_c v_\theta + v_r\right) - P, \\
\sigma_{\varphi\varphi} &= (2\eta/sr)\left(\partial_\varphi v_\varphi + sv_r + cv_\theta\right) - P, \quad \sigma_{r\theta} = (\eta/r)\left(r\partial_r v_\theta - v_\theta - s\partial_c v_r\right), \\
\sigma_{r\varphi} &= (\eta/sr)\left(sr\partial_r v_\varphi - sv_\varphi + \partial_\varphi v_r\right), \quad \sigma_{\varphi\theta} = (\eta/sr)\left(-s^2\partial_c v_\varphi + \partial_\varphi v_\theta - cv_\varphi\right).
\end{aligned} \qquad (3.2)$$

In view of (2.2) we need the off-diagonal components $\sigma_{r\theta}$ and $\sigma_{\varphi\theta}$. The above relations are valid in each of the fluid phases, albeit with different viscosities η_1 and η_2.

We write the fluid velocity as the sum of two terms,

$$\boldsymbol{v} = \boldsymbol{v}^I + \boldsymbol{v}^P, \qquad (3.3)$$

the first of which accounts for the source field (2.6) with the boundary condition (2.7). This field fully describes the Marangoni flow induced by a pointlike heat source. For a particle of finite size, the second term $\boldsymbol{v}^P$ is required in order to assure the no-slip condition at its surface. This is achieved by chosing $\boldsymbol{v}^P$ such that it satisfies both (2.7) and (2.8), yet does not contribute to the Marangoni stress.

4. Interface contribution v^I

Since the Marangoni stress (2.6) results in a jump of the velocity derivatives, the velocity is not analytic at the interface. The isotropic component of σ^M varies with the distance as $1/r^2$, and the dipolar contribution as $1/r^3$. This implies that $\boldsymbol{v}^I$ consists of axially symmetric and dipolar terms proportional to $1/r$ and $1/r^2$, respecively.

4.1. Axisymmetric part

The Marangoni flow of a heat source at the origin is obtained from the stream function $\psi = -Uacr(1\mp c)$ with the velocity scale U,

$$v_r^I = \frac{\partial_\theta\psi}{sr^2} = U\frac{a}{r}\left(1\mp 2c\right), \quad v_\theta^I = -\frac{\partial_r\psi}{sr} = U\frac{a}{r}\frac{cs}{1\pm c}. \qquad (4.1)$$

Both radial and polar components are proportional to the inverse distance; v_θ^I diverges on the positive z-axis for the minus sign, and on the negative one for the plus sign.

4.2. Dipolar part

We look for solutions of Stokes' equation that vary with distance as r^{-2} and that are singular at $c = \pm 1$. With the coordinates defined in Fig. 1, it is clear that that radial and polar components are proportional to $\cos\varphi$, and $v_\varphi^I \propto \sin\varphi$. Thus we have

$$v_r^I = f_r(c)\frac{\cos\varphi}{r^2}, \quad v_\theta^I = f_\theta(c)\frac{\cos\varphi}{r^2}, \quad v_\varphi^I = f_\varphi(c)\frac{\sin\varphi}{r^2}, \quad P^I = f_P(c)\frac{\cos\varphi}{r^3}. \qquad (4.2)$$

Inserting this ansatz in (3.1) results in four coupled equations for the functions $f_i(c)$; the incompressibility condition involves f_θ and f_φ only.

By successive elimination we obtain a single fourth-order differential equation for f_θ,

$$\partial_c^3 (1 - c^2)^2 \partial_c f_\theta = 0. \tag{4.3}$$

From its solution one readily constructs the remaining components and the related pressure; discarding regular and logarithmic terms we have

$$f_\theta = \frac{t_2 + t_3 c}{1 - c^2}, \quad f_r = \frac{t_2 c^3 + t_3}{\sqrt{1 - c^2}}, \quad f_\varphi = \frac{t_2 c + t_3}{1 - c^2}, \quad f_P = 2 t_2 c \sqrt{1 - c^2} \tag{4.4}$$

with coefficients t_2 and t_3. Note that the velocity field diverges along the vertical axis $c = \pm 1$.

4.3. *Velocity field and stress in the upper and lower halfspaces*

In view of the stress jump (2.6) it is clear that the velocity above and below the interface cannot be given in closed form. Analytic solutions in the halfspaces $c \gtrless 0$ are obtained by putting

$$t_2 = \mp t_3.$$

Then the singular factors in (4.4) disappear, and the relevant solution is given by

$$v_r^I = U \frac{1 \mp 2c}{\hat{r}} + \left(t_3 \frac{1 \mp c^3}{s} \mp t_4 sc \right) \frac{\cos \varphi}{\hat{r}^2}, \tag{4.5a}$$

$$v_\theta^I = U \frac{sc}{\hat{r}(1 \pm c)} \mp \left(\frac{t_3}{1 \pm c} - t_5 \right) \frac{\cos \varphi}{\hat{r}^2}, \tag{4.5b}$$

$$v_\varphi^I = \left(\frac{t_3}{1 \pm c} \mp t_5 c \right) \frac{\sin \varphi}{\hat{r}^2}, \tag{4.5c}$$

with $\hat{r} = r/a$ and where the plus and minus signs are valid in the upper and lower halfspaces, respectively. The axisymmetric part corresponds to (4.1), whereas the terms proportional to t_3 are obtained from (4.4). The contributions with t_4 and t_5 are well-known regular flow patterns (Schmitz & Felderhof 1982) that have been added in order to meet the boundary conditions at the interface.

The velocity field is symmetric with respect to the interface plane and continuous at $c = 0$, yet its derivatives are not and lead to a stress discontinuity along the interface. Finally, the corresponding pressure reads as

$$P^I = \mp 2\eta a \left(U \frac{c}{r^2} + (t_4 - t_3) a \frac{sc}{r^3} \cos \varphi \right). \tag{4.5d}$$

The pressure vanishes at $c = 0$ and thus is continuous at the interface. Since the viscosity η in general takes different values in the upper and lower phases, the normal component of the pressure gradient is discontinuous.

Now we determine the parameters U and t_i from the boundary conditions. In view of (2.7) for the normal velocity component we put $c = 0$ and find

$$t_5 = t_3.$$

From (3.2) we calculate the off-diagonal stress components $\sigma_{r\theta}$ and $\sigma_{\varphi\theta}$ at both sides of the interface. Their difference $\boldsymbol{\sigma}^M = \boldsymbol{\sigma}^{(1)} - \boldsymbol{\sigma}^{(2)}$ is proportional to the sum of the viscosities $\bar{\eta} = \eta_1 + \eta_2$,

$$\sigma_{r\theta}^M = -2\bar{\eta} a \frac{U}{r^2} - \bar{\eta} a^2 \frac{t_4}{r^3}, \qquad \sigma_{\theta\varphi}^M = -2\bar{\eta} a^2 \frac{t_3}{r^3}.$$

Inserting the temperature gradient in the boundary conditions (2.6), one readily obtains the velocity scale U and the remaining coefficients t_i,

$$U = -\frac{\gamma_T Q}{4\pi \bar{\eta} \bar{\kappa} a}, \quad t_3 = \frac{b}{a} U, \quad t_4 = 4\frac{b}{a} U. \tag{4.6}$$

(For a liquid-air interface one has $\bar{\eta} = \eta_1$ and $\bar{\kappa} = \kappa_1$.) Then the velocity field reads

$$v_r^I = U\frac{a}{r}\left(1 \mp 2c + \frac{b}{r}\frac{1 \mp c^3 \mp 4cs^2}{s}\cos\varphi\right), \tag{4.7a}$$

$$v_\theta^I = U\frac{a}{r}\left(\frac{cs}{1 \pm c} + \frac{b}{r}\frac{c}{1 \pm c}\cos\varphi\right), \tag{4.7b}$$

$$v_\varphi^I = U\frac{ab}{r^2}\left(\frac{1}{1 \pm c} \mp c\right)\sin\varphi, \tag{4.7c}$$

where the upper and lower signs occur in the upper and lower halfspaces, respectively. The corresponding pressure

$$P^I = \mp 2aU\eta\left(\frac{c}{r^2} + 3b\frac{sc}{r^3}\cos\varphi\right) \tag{4.8}$$

is proportional to $c = \cos\theta$ and thus vanishes at the interface.

Eqs. (4.7) and (4.8) constitute the solution for a pointlike interface particle carrying temperature monopole and dipole moments. The latter results in a radial flow velocity at the interface proportional to $r^{-2}\cos\varphi$.

4.4. Stress and force balance

From elementary symmetry considerations it is clear that both contributions to (2.5) have finite components along the x-axis only. Thus the contact line element ds reduces to the component $ds_x = ad\varphi\cos\varphi$, and the non-uniform interface tension leads to a net force $\oint ds_x \gamma$. The drag force exerted on the surface element $dS = a^2 dc d\varphi$ is given by the stress component σ_{rx}^I; from (3.2) and (4.7) one finds

$$\frac{\sigma_{rx}^I}{\eta U/a} = \left(\frac{-2s}{1 \pm c} \pm 6sc\right)\cos\varphi + \frac{b}{a}\left(\frac{-4}{1 \pm c} \pm 22c \mp 24c^3\right)\cos^2\varphi + \frac{b}{a}\left(\frac{4}{1 \pm c} \mp 6c\right)\sin^2\varphi.$$

Integrating the linearized tension $\gamma = \gamma_0 + \gamma_T(T - T_0)$ along the contact line and the stress over the particle surface, we find that the tension and drag forces cancel each other,

$$\oint ds_x \gamma + \oint dS\sigma_{rx}^I = -2\pi\bar{\eta}bU + 2\pi\bar{\eta}bU = 0. \tag{4.9}$$

5. Particle contribution v^P

Now we turn to the additional velocity v^P which is required in order to satisfy the stick boundary condition (2.8) at the particle surface,

$$u = v^I|_P + v^P|_P. \tag{5.1}$$

In addition, v^P has continuous derivatives and its normal component vanishes at the phase boundary. In other words, v^P does not contribute to the Marangoni stress (2.6) and satisfies the condition (2.7).

We start from the general analytic solution of Stokes' equation (3.1) which is given by

the well-known series (Schmitz & Felderhof 1982)

$$v_r^P = U \sum_{n,m} \frac{a^n}{r^n} \left(p_{nm} + q_{nm} \frac{a^2}{r^2} \right) X_{nm}, \tag{5.2a}$$

$$v_\theta^P = U \sum_{n,m} \left[\frac{a^n}{r^n} \left(\frac{n-2}{n(n+1)} p_{nm} + \frac{q_{nm}}{n+1} \frac{a^2}{r^2} \right) s \partial_c X_{nm} + \frac{a^{n+1}}{r^{n+1}} s_{nm} \frac{\partial_\varphi X_{nm}}{s} \right] \tag{5.2b}$$

$$v_\varphi^P = U \sum_{n,m} \left[-\frac{a^n}{r^n} \left(\frac{n-2}{n(n+1)} p_{nm} + \frac{q_{nm}}{n+1} \frac{a^2}{r^2} \right) \frac{\partial_\varphi X_{nm}}{s} + \frac{a^{n+1}}{r^{n+1}} s_{nm} s \partial_c X_{nm} \right] \tag{5.2c}$$

where $n = 1, 2, 3, \dots$ and $-n \leqslant m \leqslant n$. The angle-dependent basis functions

$$X_{nm}(c, \varphi) = \begin{cases} P_n^m(c) \cos(m\varphi) & \text{for} \quad m \geqslant 0, \\ P_n^m(c) \sin(m\varphi) & \text{for} \quad m < 0, \end{cases}$$

involve associated Legendre polynomials,

$$P_n^m(c) = \frac{(-s)^m}{2^n n!} \partial_c^{n+m} (c^2 - 1)^n,$$

for example $P_1^1 = -s$, $P_1^{-1} = s/2$, and $P_2^1 = 3sc$. The inhomogeneous solutions with coefficients p_{nm} are related to the pressure

$$P^P = 2\eta U \sum_{n,m} \frac{a^n}{r^{n+1}} \frac{2n-1}{n+1} p_{nm} X_{nm}, \tag{5.3}$$

Since the source comprises monopole and dipole moments only, the above series has finite terms with $n = 1, 2, 3, \dots$ and $m = -1, 0, 1$.

5.1. *Drag force and interface boundary conditions*

The only components that contribute to the drag force are the Stokeslet terms p_{1m}, with $m = -1, 0, 1$. Here we are interested in the force along the x-axis and thus retain the coefficient p_{11} only. The relevant component of the stress tensor reads

$$\sigma_{rx}^P = 3 p_{11} (\eta U/a) \left(1 - c^2 \right) \cos^2 \varphi.$$

In view of (2.5) and (4.9), it is clear that the surface integral of σ_{rx}^P vanishes,

$$\oint \mathrm{d}S \sigma_{rx}^P = 2\pi p_{11} \bar{\eta} a U = 0. \tag{5.4}$$

In physical terms this means that there is no additional drag force arising from σ_{rx}^P and thus no Stokeslet contribution to the flow $\boldsymbol{v}^P$.

In order not to interfere with the above solution $\boldsymbol{v}^I$ and the conditions (2.6) and (4.7), the additional term $\boldsymbol{v}^P$ satisfies

$$v_\theta^P|_I = 0, \quad \sigma_{r\theta}^P|_I = 0, \quad \sigma_{\theta\varphi}^P|_I = 0. \tag{5.5}$$

Putting $c = 0$ in both velocity and stress components, one finds that all coefficients vanish except for

$$p_{2n,0}, \quad q_{2n,0}, \quad p_{2n+1,1}, \quad q_{2n-1,1}, \quad s_{2n,-1},$$

with $n = 1, 2, 3, \dots$ These coefficients are determined from the boundary condition at the particle surface (4.7).

5.2. Axisymmetric part

We consider the velocity contributions that do not depend on the azimuthal angle φ. Inserting the velocity field $\boldsymbol{v}^P$ in (5.1), we find that the even coefficients $p_{2n,0}$ and $q_{2n,0}$ are determined by the axisymmetric part of v_r and v_θ, according to

$$0 = (1 \mp 2c) + \sum_{k \text{ even}} (p_{k0} + q_{k0}) P_k, \quad 0 = \frac{c}{1 \mp c} + \sum_{k \text{ even}} \frac{(k-2)p_{k0} + kq_{k0}}{k(k+1)} s\partial_c P_k. \quad (5.6)$$

Expanding these equations in terms of Legendre polynomials one obtains

$$q_{2n,0} = \frac{(-1)^n(4n+1)(2n)!}{2^{2n+1}n!(n+1)!}, \qquad p_{2n,0} = -\frac{2n+1}{2n-1}q_{2n,0}. \quad (5.7)$$

The coefficient p_{20} provides the leading term in inverse powers of distance, $\boldsymbol{v}^P \propto r^{-2}$. Thus $\boldsymbol{v}^P$ decays faster than the Marangoni flow $\boldsymbol{v}^I \propto r^{-1}$.

5.3. Dipolar part.

Now we turn to the dipolar terms $m = \pm 1$ in $\boldsymbol{v}^P$. Performing the derivatives with respect to φ, separating factors of $\cos\varphi$ and $\sin\varphi$, and dividing by the velocity scale U, we obtain from Eq. (5.1) the relations

$$\frac{u}{U}s = \frac{b}{a}\frac{1 \mp c^3 \mp 4cs^2}{s} + \sum_{k \text{ odd}} (p_{k1} + q_{k1}) P_k^1, \qquad (5.8a)$$

$$\frac{u}{U}c = \frac{b}{a}\frac{c}{1 \pm c} + \sum_{k \text{ odd}} \frac{(k-2)p_{k1} + kq_{k1}}{k(k+1)} s\partial_c P_k^1 + \sum_{k \text{ even}} s_{k,-1}\frac{P_k^{-1}}{s}, \qquad (5.8b)$$

$$-\frac{u}{U} = \frac{b}{a}\frac{1 \mp c - c^2}{1 \pm c} + \sum_{k \text{ odd}} \frac{(k-2)p_{k1} + kq_{k1}}{k(k+1)}\frac{P_k^1}{s} + \sum_{k \text{ even}} s_{k,-1}s\partial_c P_k^{-1}, \quad (5.8c)$$

where the upper and lower signs are valid in the halfspaces $c > 0$ and $c < 0$, respectively.

The first equation is solved by expanding in terms of the polynomials P_k^1,

$$-\frac{u}{U}\delta_{k1} = \frac{b}{a}B_k + (p_{k1} + q_{k1}) \quad (k \text{ odd}). \qquad (5.9)$$

We have used $P_1^1 = -s$ and the coefficients

$$B_{2n-1} = \frac{\int \mathrm{d}c P_{2n-1}^1(c)[1 \mp c^3 \mp 4cs^2]/s}{\int \mathrm{d}c P_{2n-1}^1(c)^2} = \frac{(-1)^n(2n)!(8n^2 - 4n - 3)}{2^{2n}n!(n+1)!(2n-1)(2n-3)},$$

with $n = 1, 2, 3, \ldots$ The first terms read $B_1 = \frac{3}{8}$, $B_3 = \frac{49}{96}$, $B_5 = -\frac{209}{1920}$.

The second and third equations in (5.8) can be conveniently separated in two parts, one that relates u/U to the coefficients p_{k1} and q_{k1}, and a second one relating the terms proportional to b/a to the coefficients $s_{k,-1}$,

$$\frac{u}{U}\delta_{k1} = \frac{(k-2)p_{k1} + kq_{k1}}{k(k+1)}, \qquad 0 = -\frac{b}{a}\frac{c}{1 \pm c} + \sum_{k \text{ even}} s_{k,-1}\frac{P_k^{-1}}{s}. \qquad (5.10)$$

For $k \geqslant 2$ equations (5.9) and (5.10) are readily solved,

$$p_{k1} = -\frac{b}{a}\frac{k}{2}B_k, \quad q_{k1} = \frac{b}{a}\frac{k-2}{2}B_k. \qquad (5.11)$$

The coefficients $s_{2n,-1}$ are determined by multiplying the second equation in (5.10) with

s and expanding in terms of $P_{k,-1}$; thus we obtain

$$s_{2n,-1} = \frac{b}{a} \frac{(-1)^n (2n-2)!(4n+1)}{2^{2n-1}(n-1)!(n+1)!}. \tag{5.12}$$

Now we turn to the case $k = 1$. Noting $p_{11} = 0$ and $B_1 = \frac{3}{8}$ one readily determines the coefficient

$$q_{11} = -\frac{2}{3} B_1 \frac{a}{b} = -\frac{a}{4b} \tag{5.13}$$

and the particle velocity

$$u = \frac{q_{11}}{2} U = -\frac{b}{8a} U. \tag{5.14}$$

It is worth noting that the coefficient q_{11} corresponds to the amplitude of the "source-doublet" of a diagrammatic expansion (Blake & Chwang 1974). The factor $-\frac{b}{8a}$ could be obtained equally well from the reciprocal theorem developed by Masoud & Stone (2014).

6. Discussion

6.1. *Velocity field in the surrounding fluid*

The total velocity field consists of two contributions, $\boldsymbol{v}^I$ and $\boldsymbol{v}^P$, which describe the long-range behavior and the flow in the vicinity of the trapped particle, respectively. The first one is entirely determined by the temperature field (2.1), whereas the second one depends on the particle size and shape. The dipolar part of the Marangoni flow (4.7) behaves as $\boldsymbol{v}^I \propto r^{-2}$, whereas to leading order $\boldsymbol{v}^P$ decays as r^{-3} and is given by the coefficients $q_{11}, p_{31}, s_{2,-1}$, which comprise the "source-doublet" of a diagrammatic expansion (Blake & Chwang 1974). In an alternative approach, the first contributions to $\boldsymbol{v}^P$ could be constructed in terms of an image system by successive reflections at the particle surface and at the interface (Morthomas & Würger 2010).

The dipolar component of the Marangoni flow varies with the square of the inverse distance, $\boldsymbol{v}^I \propto r^{-2} \cos\varphi$. This power law is related to the fact heat or a molecular solute diffuse in a bulk phase, and that temperature or concentration obey the 3D diffusion equation. On the other hand, a surfactant diffuses along the 2D interface only, and the resulting Marangoni flow behaves as $r^{-1} \cos\varphi$ (Lauga & Davis 2012).

Throughout this paper we have assumed that the interface plane coincides with the particle's midplane, requiring the contact angle $\theta_0 = \pi/2$. As a consequence, the velocity field $\boldsymbol{v}(\boldsymbol{r})$ is perfectly symmetric with respect to the interface. In the general case $\theta_0 \neq \pi/2$, the particle center is above or below the interface. Then the Marongoni flow $\boldsymbol{v}^I$ is still symmetric, whereas the contribution arising from the boundary condition at the particle surface, $\boldsymbol{v}^P$, is no longer the same above and below the interface. This would double the number of independent coefficients in the boundary conditions at the particle surface and modify the numerical factor in (5.14). We do not expect a change of the qualitative results; in particular the far-field $\boldsymbol{v}^I$ is not affected by the vertical particle position.

6.2. *Single-particle velocity*

According to (5.14) a non-uniformly heated colloidal sphere moves in the direction opposite to its self-generated temperature gradient. With U from Eq. (4.6), the self-propulsion velocity is given by the tension derivative γ_T, the particle's heat absorption rate Q and dipole moment b, and the fluid viscosity $\bar{\eta}$ and heat conductivity $\bar{\kappa}$. In terms of the

excess temperature at the particle surface, $\Delta T = Q/2\pi\bar{\kappa}a$, the velocity scale reads as

$$U = -\frac{\gamma_T \Delta T}{2\bar{\eta}}. \tag{6.1}$$

With the parameters of a water-air interface at room temperature, $\bar{\eta} = 10^{-3}$ Pa.s and $\gamma_T = -2\times10^{-3}$ NK^{-1}m^{-1}, we find that hot particles with an excess temperature $\Delta T = 1$ K induce a Marangoni flow with velocity scale U of the order of 1 m/s.

The self-propulsion velocity u then depends on the reduced temperature dipole moment b/a. For a particle that is heated through laser-absorbing molecules dispersed in the particle's bulk material, the asymmetry b/a is significantly smaller than unity. On the other hand, if the heating occurs through a metal patch fixed on its surface, one has $b/a \approx 1$ and $u \approx -\frac{1}{10}U$. This estimate agrees qualitatively with the velocity of several cm/s observed by Okawa et al. (2009) for a macroscopic floater with a hot spot at one side. Note that, at constant excess temperature, U is independent of the particle size.

6.3. *Non-linear effects*

The stationary temperature profile (2.1) accounts for diffusive heat flow from an immobile source but neglects convective transport and the particle's motion. This approximation is valid for small Marangoni number aU/α, where α is the thermal diffusivity. For micron-size particles and $\alpha = 1.4 \times 10^{-7}$ m^2/s for water, one find that the linear approximation ceases to be valid at $U \approx 10$ cm/s. In the case of a chemical Marangoni effect, the relevant parameter is provided by the Péclet number aU/D of the molecular solute with diffusivity D. Since molecules diffuse more slowly than heat (D is about hundred times smaller than α), the linear approximation is restricted to velocities $U \sim$ mm/s. Finally, convective acceleration is negligible for small Reynolds number aU/ν, with the kinematic viscosity ν; this condition holds true for $U < 1$ m/s.

We briefly discuss two non-linear effects, heat advection by the fluid velocity and distortion of the temperature field due to the particle motion. The temperature profile of an immobile heat source is determined by $\partial_t T = \boldsymbol{\nabla}\cdot(T\boldsymbol{v} - \alpha\boldsymbol{\nabla}T)$. For small Marangoni number the advective term is negligible, and the excess temperature varies with the inverse distance. For $aU/\alpha > 1$ advection enhances the heat flow and modifies the temperature profile in the vicinity of the particle ($r < \alpha/U$).

An additional effect occurs at finite particle velocity u, where heat diffusion is efficient at short distances only, thus resulting in strong retardation effects in the far-field. For a hot particle moving in negative x-direction, the $1/r$ term of (2.1) is distorted according to

$$T(r) = T_0 + \frac{Q}{2\pi\bar{\kappa}r}e^{-(r-x)/\ell}, \tag{6.2}$$

with $\ell = -\alpha/u$. At large distances ($r > \ell$), the diffusive heat transport does not catch up the particle's motion, resulting in an asymmetric temperature profile that decays more rapidly in front of the moving particle ($x < 0$) and thus significantly modifies the Marangoni stress (2.2).

6.4. *Collective effects*

We conclude with a brief discussion of collective effects arising from the interplay of self-propulsion and hydrodynamic interactions; the latter are well approximated by the far-field contribution $\boldsymbol{v}^I$. In addition to the self-generated velocity $\boldsymbol{u}_i = -u\boldsymbol{e}_i$, each particle is advected in the Marangoni flow of its neighbors $\boldsymbol{w}_i$, resulting in the drift-diffusion

equation for the probability density $\rho(\boldsymbol{r}, \boldsymbol{e})$,

$$\partial_t \rho + \hat{\boldsymbol{\nabla}} \cdot (\boldsymbol{u} + \boldsymbol{w})\rho = D\hat{\boldsymbol{\nabla}}^2 \rho + D_r \mathcal{R}^2 \rho, \tag{6.3}$$

with the 2D gradient $\hat{\boldsymbol{\nabla}}$, the rotation operator about the vertical axis $\mathcal{R} = \boldsymbol{e} \times \partial_{\boldsymbol{e}}$, and the diffusion coefficients D and D_r. The self-generated Marangoni flow of spheres does not exert a viscous torque, in contrast to sufficiently asymmetric particles Nakata et al. (1997) and in contrast to the effective slip velocity in bulk phases (Bickel 2014); the torque exerted by the vorticity of the advection flow is small.

Evaluating (4.7) at the interface, one readily obtains the advection velocity as a gradient field $\boldsymbol{w}_i = -\hat{\boldsymbol{\nabla}}_i \Phi_i$, where the effective single-particle potential

$$\Phi_i = aU \sum_j \left(-\ln r_{ij} + \frac{\boldsymbol{b}_j \cdot \boldsymbol{r}_{ij}}{r_{ij}^2} \right), \tag{6.4}$$

depends on the distance vector $\boldsymbol{r}_{ij} = \boldsymbol{r}_j - \boldsymbol{r}_i$ and the temperature dipole $\boldsymbol{b}_j = b\boldsymbol{e}_j$ of the neighbor j.

For $b \approx 0$ both the self-propulsion velocity $\boldsymbol{u}$ and the dipole term in Φ_i are small. For chemically active particles, Eq. (6.3) leads to the Keller-Segel model and its rich dynamical behavior (Masoud & Shelley 2014). For an external source field, such as the excess temperature due to laser heating of absorbing particles, an outward Marangoni flow ($U > 0$) results in a radially symmetric repulsive pair interaction, and the steady state $\rho_{\text{st}} \propto e^{-\Phi/D}$ is given by the effective overall potential $\Phi = -aU \sum_{<i,j>} \ln r_{ij}$. This potential favors an ordered phase of hexatic symmetry, which was indeed observed for camphor boats floating on water (Soh et al. 2008).

A more complex behavior is expected for a non-zero temperature dipole b. During its rotational diffusion time the particle travels over a distance $L = u/D_r$. If this length is smaller than the nearest-neighbor distance d of the hexatic lattice, self-propulsion merely enhances the effective diffusion coefficient (Howse et al. 2007). With a rotational diffusion time of $1/D_r \approx 5$ s, micron-size particles may attain a velocity u of several mm/s, resulting in a length L of several centimeters. Then the self-generated motion destroys the hexatic lattice and may lead to disordered phases where the particle orientations $\boldsymbol{e}_i$ play the role of quenched random fields.

REFERENCES

BICKEL, T., MAJEE, A., WÜRGER, A. 2013 Flow pattern in the vicinity of self-propelling hot Janus particles. *Phys. Rev. E* **88**, 01230

BICKEL, T., ZECUA, G., WÜRGER, A. 2014 Polarization of active Janus particles. *Phys. Rev. E* **89**, 050303(R)

BLAKE, J.R., CHWANG, A.T. 1974 Fundamental singularities of viscous flow. *J. Eng. Math.* **8**, 23

BRENNER, H. 1961 The slow motion of a sphere through a viscous fluid towards a plane surface. *Chem. Eng. Sci.* **16**, 242

HOWSE, J.R., JONES, R.A.L., RYAN, A.J., GOUGH, T., VAFABAKHSH, R. GOLESTANIAN, R. 2007 Self-Motile Colloidal Particles: From Directed Propulsion to Random Walk. *Phys. Rev. Lett.* **99**, 048102.

LAUGA, E., DAVIS, A.M. 2012 Viscous Marangoni propulsion. *J. Fluid Mech.* **705**, 120

MASOUD, H., SHELLEY, M. 2014 Collective surfing of chemically active particles. *Phys. Rev. Lett.* **112**, 128304

MASOUD, H., STONE, H.A. 2014 A reciprocal theorem for Marangoni propulsion. *J. Fluid. Mech.* **741**, R4

MORTHOMAS, J., WÜRGER, A. 2010 Hydrodynamic attraction of immobile particles due to interfacial forces. *Phys. Rev. E* **81**, 051405

NAGAI, K.H., TAKABATAKE, F., SUMINO, Y., KITAHATA, H., ICHIKAWA, M., YOSHINAGA, N. (2013) Rotational motion of a droplet induced by interfacial tension. *Phys. Rev. E* **87**, 013009.

NAKATA, S., IGUCHI, Y., OSE, S., KUBOYAMA, M., ISHII, T., YOSHIKAWA, K. 1997 Self-Rotation of a Camphor Scraping on Water: New Insight into the Old Problem. *Langmuir* **13**, 4454.

OKAWA, D., PASTINE, S.J., ZETTL, A., FRÉCHET, J.M.J. 2009 Surface Tension Mediated Conversion of Light to Work. *J. Am. Chem. Soc.* **131**, 5396-5398.

PAXTON, W.F., SEN, A., MALLOUK, T.E. (2005) Motility of Catalytic Nanoparticles through Self-Generated Forces. *Chem. Eur. J.* **11**, 6462

QIAN, B., MONTIEL, D., BREGULLA, A., CICHOS, F., YANG, H. 2013 Harnessing thermal fluctuations for purposeful activities: the manipulation of single micro-swimmers by adaptive photon nudging. *Chem. Sci.* **4**, 1420.

ROBERT DE SAINT VINCENT, M., DELVILLE, J.-P. 2012 Microfluidic Transport Driven by Opto-Thermal Effects, in KELLY, R.T. (ED.) *Advances in Microfluidics* ISBN 978-953-51-0106-2, Publisher: InTech

SCHMITZ, R., FELDERHOF, B.U. 1982 *Physica* **113A**, 90

SOH, S., BISHOP, K.J.M., GRZYBOWSKI, B.A. 2008 Dynamic Self-Assembly in Ensembles of Camphor Boats. *J. Phys. Chem. B* **112**, 10848.

VENANCIO-MARQUES, A., BARBAUD, F., BAIGL, D. 2013 Microfluidic Mixing Triggered by an External LED Illumination. *J. Am. Chem. Soc.* **135**, 3218.